Bioorganic & Medicinal Chemistry 19 (2011) 3757–3768

Contents lists available at ScienceDirect

Bioorganic & Medicinal Chemistry

journal homepage: www.elsevier.com/locate/bmc

Synthesis, structure–affinity relationships, and molecular modeling studies of novel pyrazolo[3,4-*c*]quinoline derivatives as adenosine receptor antagonists

Ombretta Lenzi [a], Vittoria Colotta [a,*], Daniela Catarzi [a], Flavia Varano [a], Lucia Squarcialupi [a], Guido Filacchioni [a], Katia Varani [b], Fabrizio Vincenzi [b], Pier Andrea Borea [b], Diego Dal Ben [c], Catia Lambertucci [c], Gloria Cristalli [c]

[a] *Dipartimento di Scienze Farmaceutiche, Laboratorio di Progettazione, Sintesi e Studio di Eterocicli Biologicamente Attivi, Universita' di Firenze, Polo Scientifico, Via Ugo Schiff 6, 50019 Sesto Fiorentino, FI, Italy*
[b] *Dipartimento di Medicina Clinica e Sperimentale, Sezione di Farmacologia, Università di Ferrara, Via Fossato di Mortara 17-19, 44100 Ferrara, Italy*
[c] *School of Pharmacy, Medicinal Chemistry Unit, University of Camerino, Via S. Agostino 1, 62032 Camerino (MC), Italy*

ARTICLE INFO

Article history:
Received 21 February 2011
Revised 28 April 2011
Accepted 1 May 2011
Available online 6 May 2011

Keywords:
G protein-coupled receptors
Adenosine receptor antagonists
Pyrazoloquinolines
Tricyclic heteroaromatic systems
Ligand-receptor modeling studies

ABSTRACT

This paper reports the study of new 2-phenyl- and 2-methylpyrazolo[3,4-*c*]quinolin-4-ones (series **A**) and 4-amines (series **B**), designed as adenosine receptor (AR) antagonists. The synthesized compounds bear at the 6-position various groups, with different lipophilicity and steric hindrance, that were thought to increase human A_1 and A_{2A} AR affinities and selectivities, with respect to those of the parent 6-unsubstituted compounds. In series **A**, this modification was not tolerated since it reduced AR affinity, while in series **B** it shifted the binding towards the hA_1 subtype. To rationalize the observed structure–affinity relationships, molecular docking studies at A_{2A}AR-based homology models of the A_1 and A_3 ARs and at the A_{2A}AR crystal structure were carried out.

1. Introduction

Adenosine is an ubiquitous nucleoside which affects a wide range of physiopathological processes by activation of G protein-coupled receptors, currently subdivided into four subtypes: A_1, A_{2A}, A_{2B}, and A_3. Each receptor subtype mediates distinct pharmacological actions through coupling to various secondary effectors. Adenylate cyclase can be considered the principal effector system, common to all ARs. It can be either inhibited (A_1 and A_3) or stimulated (A_{2A} and A_{2B}) thus decreasing or increasing, respectively, cAMP production.[1,2] Other second messenger signaling pathways have also been described.[1–3] The A_1 receptor activates phospholipase C, leading to increased production of inositol 1,4,5-triphosphate and Ca^{2+} mobilization; the A_1 subtype is also known to modulate several types of K^+ and Ca^{2+} channels that are, respectively, activated or inactivated. The A_{2A}AR is recognized to activate protein kinase C, K_{ATP} and Ca^{2+} channels. Both A_1 and A_{2A} ARs regulate the extracellular signal-regulated kinases (ERK) 1/2, members of the mitogen-activated protein kinase (MAPK) family that play an important role in cell differentiation, survival, proliferation and death.[1,4,5] ARs exhibit different tissue/cell distribution.[1,3] A_1 ARs are abundant within the central nervous system, with high levels being expressed in many regions of the brain, such as cerebral and cerebellar cortex, hippocampus, thalamus, and limbic region. A_1 ARs are localized at post-synaptic level and also on pre-synaptic terminals; activation of these latter A_1 ARs inhibits glutamatergic and cholinergic transmission. Thus, A_1 AR blockade can increase the release of acetylcholine and glutamate in brain areas which are important for cognitive and emotional functions. Coherently, A_1 AR antagonists ameliorate cognitive deficits due to cholinergic hypofunction and have potential for the treatment of neurological disorders, such as dementia or anxiety.[6] Also A_{2A} ARs are expressed through the brain, showing the highest levels in the striatum, nucleus accumbens, and olfactory tubercle, regions which are rich in dopamine. A_{2A}AR inactivation in the brain explicates a neuroprotective effect, attributed to the release inhibition of glutamate and proinflammatory cytokines from microglia. A_{2A} receptor antagonists improve dopamine transmission, thus being effective in the treatment of Parkinson's disease (PD).[7] Recently, also the usefulness of dual A_{2A}/A_1 receptor antagonists in the treatment of PD has been highlighted because these compounds not only improve motor disabilities (A_{2A}AR) but also reduce the cognitive impairment (A_1AR) associated with the disease.[8,9]

On the basis of the interesting potential therapeutic applications, numerous classes of AR antagonists, with different

* Corresponding author. Tel.: +39 055 4573731; fax: +39 055 4573780.
E-mail address: vittoria.colotta@unifi.it (V. Colotta).

0968-0896/$ - see front matter © 2011 Elsevier Ltd. All rights reserved.
doi:10.1016/j.bmc.2011.05.001

heterocyclic structures, have been developed and intensive structure–affinity relationship studies have been performed.[10–15]

Also in our laboratory much research has been devoted to the study of AR antagonists, belonging to various classes of heteroaromatic tricyclic or bicyclic derivatives.[16–25] One of the tricyclic series recently investigated is represented by the 2-arylpyrazolo[3,4-*c*]quinolines, both 4-oxo and 4-amino substituted (series **A** and **B**, respectively, Fig. 1).[17,21,23]

The 2-phenyl derivatives **1A** and **1B**[21] can be considered the parent compounds of the two series: the 4-oxo derivative **1A** shows nanomolar affinities for human (h) A_3 (K_i = 30.8 nM) and A_1 (K_i = 203 nM) ARs and a scarce binding activity at the hA_{2A} AR (I% = 45, at 10 μM); instead, the 4-amino derivative **1B** binds the A_{2A}AR with high affinity (K_i = 91 nM) and is about five- to six-fold less active at A_1AR (K_i = 659 nM) and A_3AR (K_i = 551 nM) receptors (Table 1). Introduction of a small substituent on the *meta*- or *para*-position of the 2-phenyl ring of **1A** (X = Me, OMe) gave non-selective A_1/A_3 antagonists since it ameliorated both A_1AR (K_i = 12–176 nM) and A_3AR affinity (K_i = 3–30 nM); instead, the A_{2A}AR binding remain unsatisfactory (I% = 25–50 at 10 μM).[21] Also in series **B**, the X substituents increased both A_1 AR (K_i = 21–45 nM) and A_3 AR (K_i = 90–228 nM) affinity of the parent compound **1B**, thus leading to non-selective antagonists. On the contrary, the A_{2A} AR affinity is decreased by the presence of X, being the 2-aryl derivatives **B** from three- to ten-fold less active at the A_{2A}AR than the parent compound **1B**.[21] Based on these results, we planned the synthesis of new pyrazolo[3,4-*c*]quinolines with the aim of obtaining A_1AR selective antagonists or dual A_1/A_{2A} antagonists, due to their interesting therapeutic applications in the neurological disorders cited above. Thus, we decided to introduce at the 6-position (R) of both compounds **1A** and **1B** various groups with different steric hindrance and lipophilicity (compounds **1–11**, Fig. 2). In particular, the presence of 6-R bulky and lipophilic groups, such as bromine or arylalkyl moieties, was thought to enhance the A_1AR and A_{2A}AR affinities since literature data on several tricyclic AR antagonists of similar size and shape to our 4-amino series **B**, indicate that an arylalkyl chain in a suitable position shifted the affinity towards A_1 and/or A_{2A} ARs.[26–28] The choice of synthesizing analogues of **1A** and **1B**, lacking X substituent on the 2-phenyl moiety, was made because the presence of X groups might have been disadvantageous for the binding at the A_{2A}AR, as well as for A_1 or A_{2A} AR selectivity. Finally, the effect of replacing the 2-phenyl moiety with the smaller and less lipophilic 2-methyl group was investigated in both series **A** and **B** (compounds **12–15**, Fig. 2).

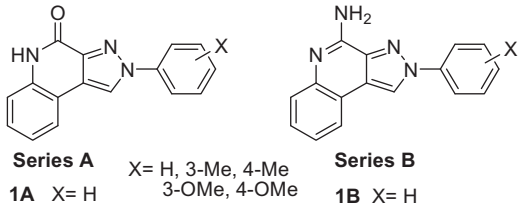

Figure 1. Previously reported 2-arylpyrazolo[3,4-*c*]quinolin-4-ones (series **A**) and 4-amines (series **B**).

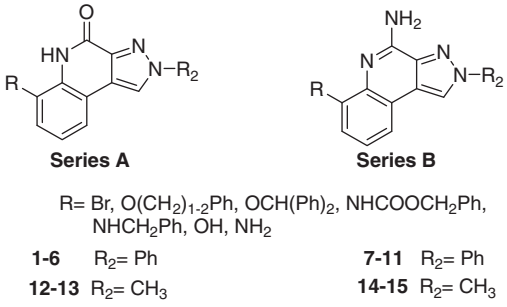

Figure 2. Herein reported 6-substituted 2-phenylpyrazolo[3,4-*c*]quinoline derivatives **1–11** and 2-methylpyrazolo[3,4-*c*]quinolines **12–15**.

2. Chemistry

The target pyrazolo[3,4-*c*]quinoline derivatives **1–15** were synthesized as depicted in Schemes 1–3. Scheme 1 shows the pathways followed to obtain the 2-phenylpyrazoloquinolin-4-one derivatives **1–6**. A mixture of the commercially available 7-benzyloxyindole **16** or the suitably synthesized 7-R indoles **17–19**,[29–31] ethoxalyl chloride and anhydrous pyridine was refluxed for two days to give the corresponding 7-R-3-ethoxalylindoles **20–21**[32,33] and **22–23**. Reaction of **20–21** with phenylhydrazine hydrochloride in refluxing absolute ethanol and a few drops of glacial acetic acid afforded the desired 6-substituted pyrazoloquinolin-4-one derivatives **1–2**. Instead, the 7-benzhydryloxyindole **22**, under the same conditions, yielded a mixture (about 1:1) of the corresponding 6-benzhydryloxy-pyrazoloquinoline **3** and of the 6-hydroxy derivative **5**, which was also prepared by debenzylation of compound **1**. Catalytic reduction of compounds **4** gave the 6-amino derivative **6**.

The 2-phenylpyrazoloquinolin-4-amino derivatives **7–11** were prepared as outlined in Scheme 2. The 4-oxo derivatives **1–2** and **4** were refluxed in a mixture of phosphorus pentachloride/phosphorus oxychloride to give the corresponding 4-chloro derivative **24–26**. Compounds **24–25** were transformed into the 4-amino substituted compounds **7–8** with ammonia. Catalytic hydrogenation of derivative **7** yielded the corresponding 6-hydroxy substituted compound **9** that was reacted with phenethyl bromide to obtain the 6-phenethyloxy-substituted derivative **10**. When the 4-cloro derivative **26** was heated with ammonia, both the 4-amino derivative **27** and the 4,6-diamino-2-phenylpyrazoloquinoline **28**

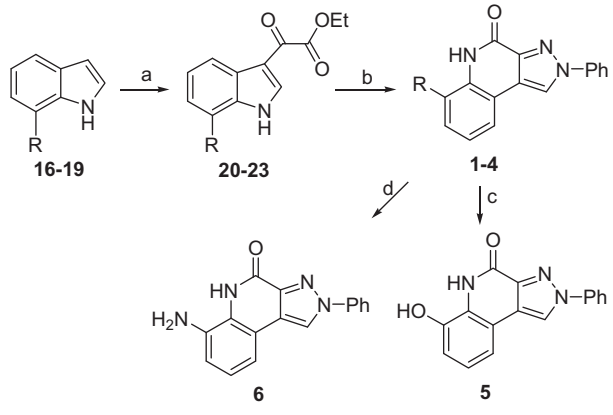

	R
1, 16, 20	OCH_2Ph
2, 17, 21	Br
3, 18, 22	$OCH(Ph)_2$
4, 19, 23	$NHCOOCH_2Ph$

Scheme 1. Reagents and conditions. (a) EtOCO–COCl, anhydrous Et_2O, reflux; (b) $PhNHNH_2$·HCl, glacial AcOH, absolute EtOH, reflux; (c) 48% HBr, AcOH, reflux; (d) H_2, Pd/C, DMF, 45 psi.

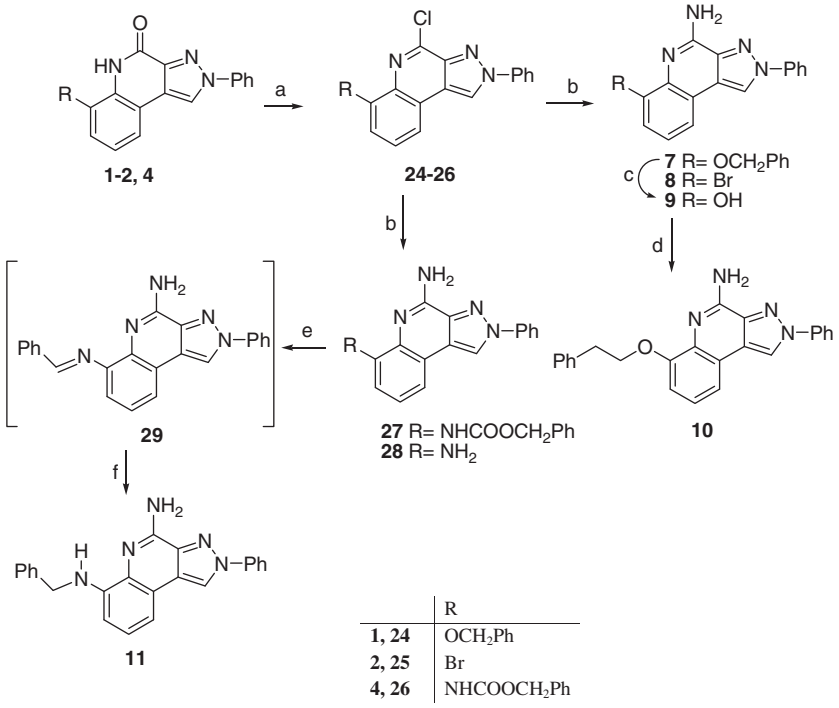

Scheme 2. Reagents and conditions. (a) $PCl_5/POCl_3$, reflux; (b) NH_3(g), absolute EtOH, $T = 120$ °C, sealed tube; (c) H_2, 10% Pd/C, 35 psi; (d) phenethyl bromide, K_2CO_3, 2-butanone, reflux; (e) PhCHO, anhydrous $ZnCl_2$, anhydrous THF, reflux; (f) $NaBH_4$, anhydrous MeOH, reflux.

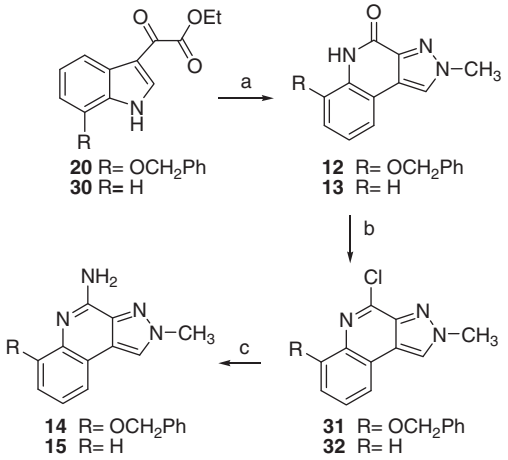

Scheme 3. Reagents and conditions. (a) $CH_3NHNH_2 \cdot HCl$, glacial AcOH, absolute EtOH, reflux; (b) $PCl_5/POCl_3$, reflux; (c) NH_3(g), absolute EtOH, $T = 110$ °C, sealed tube.

were obtained. Reaction of this latter with benzaldehyde in refluxing anhydrous tetrahydrofuran, and in the presence of anhydrous zinc chloride, afforded the Schiff's base **29** which was reduced with sodium borohydride to give the 6-benzylamino derivative **11**. The 2-methylpyrazolo[3,4-*c*]quinolin-4-ones **12**[34] and **13** (Scheme 3) were synthesized starting from the suitable 3-ethoxalylindoles **20**[32] or **30**[35] which were reacted with methylhydrazine hydrochloride in boiling absolute ethanol and a few drops of glacial acetic acid to give the desired 4-oxo derivatives **12–13**. These compounds were reacted with boiling phosphorus pentachloride/phosphorus oxychloride to give the corresponding 4-chloro derivatives **31–32** which were transformed into the target 2-methylpyrazolo[3,4-*c*]quinolin-4-amines **14** and **15**[36,37] with ammonia.

3. Pharmacology

The synthesized compounds **1–15** were tested for their ability to displace specific [^{3}H]DPCPX, [^{3}H]ZM241385 and [^{125}I]AB-MECA binding from cloned hA_1, hA_{2A} and hA_3 receptors, respectively, stably expressed in CHO cells. Compounds **1–15** were also tested at the hA_{2B} subtype by measuring their inhibitory effects on NECA-stimulated cAMP levels in CHO cells stably transfected with the hA_{2B} receptor. The results of binding experiments and cAMP assays are reported in Table 1, where hA_1, hA_{2A} and hA_3 affinities of the parent compounds **1A** and **1B** are also included as reference data.

4. Results and discussion

4.1. Structure–affinity relationships

The binding results indicate that the aim of the paper has been partially satisfied. In fact, most of the newly synthesized 6-substituted 2-phenylpyrazolo[3,4-*c*]quinolin-4-amines (series **B**) showed A_1 receptor affinity and selectivity (derivative **7–9**, and **11**). However, only one compound, the 2-methyl-6-benzyloxy derivative **14**, possesses affinity towards both A_1 and A_{2A} receptors. Moreover, it binds at the A_3 receptor subtype with comparable affinity. Quite unexpectedly, none of the 6-substituted 2-phenylpyrazolo [3,4-*c*]quinolin-4-one derivatives **1–6** (series **A**) possesses affinities towards ARs, whatever the nature of the 6 substituent. In fact, either lipophilic or hindering groups such as the benzyloxy, benzhydryloxy, benzyloxycarbamoyl or bromine (compounds **1–4**) or small hydrophilic substituents, such as hydroxyl or amino (compounds **5** and **6**), exerted a deleterious effect since they reduced the A_1 and A_3 receptor affinities of the parent compound **1A**, as well as the A_{2A} receptor binding. As stated above, the 6-substituted 2-phenylpyrazolo[3,4-*c*]quinolin-4-amino derivatives **7–11** turned out selective A_1 AR antagonists. Indeed, they are inactive at the A_{2A},

Table 1
Binding affinity (K_i) at hA_1, hA_{2A} and hA_3 ARs and potencies (IC_{50}) at hA_{2B}.

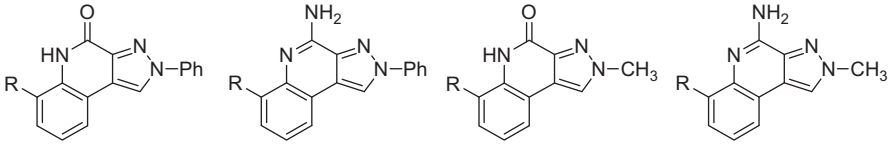

1A, 1-6 **1B, 7-11** **12-13** **14-15**

	R	Binding experiments K_i (nM) or I%			cAMP assays I%
		hA_1[b]	hA_{2A}[c]	hA_3[d]	hA_{2B}[e]
1A[f]	H	203 ± 12	43%	30.8 ± 2.6	Nt[g]
1	OCH_2Ph	20%	1%	33%	2%
2	Br	8%	17%	16%	5%
3	$OCHPh_2$	6%	1%	6%	7%
4	$NHCOOCH_2Ph$	3%	1%	14%	5%
5	OH	1%	5%	16%	4%
6	NH_2	8%	1%	18%	5%
1B[f]	H	659 ± 43	91 ± 7.3	551 ± 34	Nt[g]
7	OCH_2Ph	140 ± 12	16%	20%	5%
8	Br	300 ± 28	35%	29%	2%
9	OH	100 ± 12	19%	20%	4%
10	$O(CH_2)_2Ph$	40%	11%	28%	5%
11	$NHCH_2Ph$	455 ± 47	1%	1%	3%
12	OCH_2Ph	2%	1%	600 ± 58	3%
13	H	2%	1%	12%	2%
14	OCH_2Ph	970 ± 80	750 ± 70	500 ± 47	4%
15	H	20%	26%	18%	5%

[a] K_i values are means ± SEM of four separate assays each performed in duplicate. Percentage of inhibition (I%) are determined at 1 μM concentration of the tested compounds.
[b] Displacement of specific [^{3}H]DPCPX competition binding to hA_1CHO cells.
[c] Displacement of specific [^{3}H]ZM241385 competition binding to hA_{2A}CHO cells.
[d] Displacement of specific [^{125}I]AB-MECA competition binding to hA_3CHO cells.
[e] Percentage of inhibition on cAMP experiments in hA_{2B}CHO cells, stimulated by 200 nM NECA, at 1 μM concentration of the examined compounds.
[f] Ref. 17: I% at the A_{2A} receptor was determined at 10 μM concentration of compound **1A**.
[g] Nt: Not tested.

A_{2B} and A_3 receptors while they showed hA_1 receptor affinities in the nanomolar range (K_i = 100–455 nM), with the only exception being the 6-phenethyloxy-substituted derivative **10** that, at 1 μM concentration, inhibited the radioligand binding by only 40%.

In general, the substituents introduced at the 6-position of the parent compound **1B** enhanced the hA_1 affinity, the best being the 6-hydroxy group (compound **9**); unexpectedly, the presence of a 6-substituent, either lipophilic or hydrophilic, dramatically decreased the A_{2A} receptor binding of the parent derivative **1B**. These findings led us to presume that the lack of A_{2A} affinity of the new 2-phenyl derivatives, and in particular of the 4-amino substituted one, could be due to the great volume of the molecules which might hinder their accommodation in the receptor binding site. Thus, to reduce the steric hindrance, the 2-phenyl ring of the 6-benzyloxy derivatives **1** and **7** was replaced with a methyl group to afford derivatives **12** and **14**, respectively. The binding data of 2-methyl-4-oxo derivative **12** resembled those of the corresponding 2-phenyl-4-oxo substituted compounds **1**, with the exception of the A_3 affinity that was significantly higher (K_i = 600 nM).

Even more interesting results were obtained for the 2-methyl-4-amino derivative **14** that turned out to be a non selective AR antagonist. In fact it displayed comparable affinity for the A_1, A_{2A} and A_3 ARs, while it was inactive at the A_{2B} subtype. Therefore, replacement of the phenyl ring of compound **7** with the smaller methyl group (compound **14**) made the hA_{2A} affinity appear, as well as the A_3 one, while it reduced the binding at the A_1 receptor. Removal of the 6-benzyloxy substituent from the 2-methyl-4-amino derivative **14**, to give compound **15**, caused a drastic drop of A_1, A_{2A} and A_3 affinity that can be ascribed to the loss of interaction of the benzyl moiety with the receptor pocket or, in general, to a reduced complementarity with the receptor recognition sites. Similarly, the A_3 affinity of the 6-benzyloxy-4-oxo derivative **12** was annulled by removal of the 6-substituent (compound **13**). The roles of the 2- and 6-substituents and of the 4-oxo or amino function were investigated with molecular modeling studies.

4.2. Molecular modeling studies

To define the structural features at the base of the different binding affinities of the new derivatives, a molecular docking analysis was performed on homology models of hA_1 and hA_3 ARs, developed by using the recently published crystal structure of the hA_{2A} AR in complex with the ZM241385 antagonist (Fig. 3) as template,[38] and on the hA_{2A}AR crystal structure itself. In particular, docking analysis at the A_1 AR was aimed at rationalizing the effect of the different 2- and 6-substituents on the affinity for this AR subtype, while comparative docking analysis at the three AR subtypes was performed for compounds **1A** and **1B** to evaluate the impact of the different chemical functions in the 4-position on the AR binding. The hA_{2A} AR crystal structure allows improvement of the accuracy of AR homology models, due to the high res-

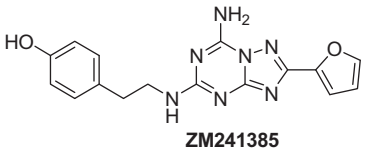

ZM241385

Figure 3. High affinity hA_{2A} AR antagonist ZM241385.

idue conservation in the primary sequences of the AR subtypes, which share a sequence identity of ~57% within the transmembrane (TM) domains.[39] The residues located within the seven TM domains in the upper part of ARs, corresponding to the ligand binding site, are conserved with an average identity of 71%.[40] Furthermore, the hA_{2A} AR crystal structure is solved in complex with the high affinity antagonist ZM241385, hence presenting a cavity suitable as binding site for docking analysis. The obtained A_1 and A_3 AR homology models were checked by using the Protein Geometry Monitor application within MOE, which provides a variety of stereochemical measurements for inspection of the structural quality in a given protein, such as backbone bond lengths, angles and dihedrals, Ramachandran φ–ψ dihedral plots, and side chain rotamer and nonbonded contact quality.

A_1, A_{2A}, and A_3 AR structures were then used as target for the docking analysis of synthesised derivatives. Due to the presence in the template crystal structure of some water molecules playing a relevant role in hA_{2A}AR-ZM241385 interaction, it was decided to reintroduce these water molecules in the hAR binding sites for the post-docking energy minimization stage, to verify possible roles of solvent molecules in stabilizing compound binding and to compare these roles to the one played for hA_{2A}R-ZM241385 interaction. All ligand structures were optimized using RHF/AM1 semi-empirical calculations and the software package MOPAC[41] implemented in MOE was utilized for these calculations. The compounds were then docked into the binding site of the ARs by using the MOE Dock tool. Top-score docking poses of each compound were subjected to energy minimization and then rescored using two available methods implemented in MOE: the *London dG* scoring function that estimates the free energy of binding of the ligand from a given pose; and *Affinity dG* Scoring that estimates the enthalpic contribution to the free energy of binding. Additional scoring was performed using the *dock-pK_i* predictor that uses the MOE *scoring.svl* script to estimate for each ligand a pK_i value, which is described by the H-bonds, transition metal interactions, and hydrophobic interactions energy. For each compound, the top-score docking pose, according to at least two out of three scoring functions, was selected for final ligand-target interaction analysis.

The docking methodology was firstly tested by comparing the predicted binding mode of ZM241385 within the A_{2A}AR pocket with respect to the X-ray data. As displayed in Figure 4, the docking method showed good ability in reproducing the ZM241385 binding mode observed in the experimental data. In particular, the RMSD of the two conformations was calculated as 1.4547 Å, with the best matching being given by the 2-(furan-2-yl)-[1,2,4]triazolo[1,5-*a*][1,3,5]triazin-7-amine moiety (0.8551 Å) and the highest deviation being given by a slightly different orientation of the 4-(2-aminoethyl)phenol group (2.1143 Å).

Considering the general binding mode of both 4-oxo and 4-amino substituted pyrazoloquinoline derivatives in the A_{2A}AR, the pyrazolo[3,4-*c*]pyridine moiety is located approximately in correspondence with the [1,2,4]triazolo[1,5-*a*][1,3,5]triazine scaffold of the co-crystallized ZM241385 antagonist. The docking conformations present the 2-substituent pointed towards the central transmembrane core and located in a mainly hydrophobic subpocket in proximity of Val84, Leu85, Met177, Trp246, and Leu249. Analogue binding motif of the pyrazoloquinoline derivatives was observed in A_1 (Fig. 5) and A_3 AR subtypes in which the hydrophobic subpockets that accommodate the 2-substituent are surrounded by Val87, Leu88, Met180, Trp247, Leu250 (A_1 AR), and Leu90 Leu91, Met177, Trp243 and Leu246 (A_3AR). In all three ARs, the 6-substituent of the new compounds is located at the entrance of the binding site. Some of the ZM241385-A_{2A}AR interactions are reproduced by the synthesised derivatives, such as the π-stacking interaction between the compound scaffold and the Phe168 residue within EL2 segment. An analogous interaction was engaged within the A_1 (Phe171) and A_3 (Phe168) ARs.

On the contrary, the double polar interaction of Asparagine 6.55 amide group (Asn253) with both the NH_2 group and the N1 atom of ZM241385 was not observed in the pyrazoloquinoline derivatives. In this series, the possible interaction of Asn 250 with both the 4-substituent and N3 atom is actually reduced to the unique interaction with the 4-group, due to the steric hindrance of 2-phenyl

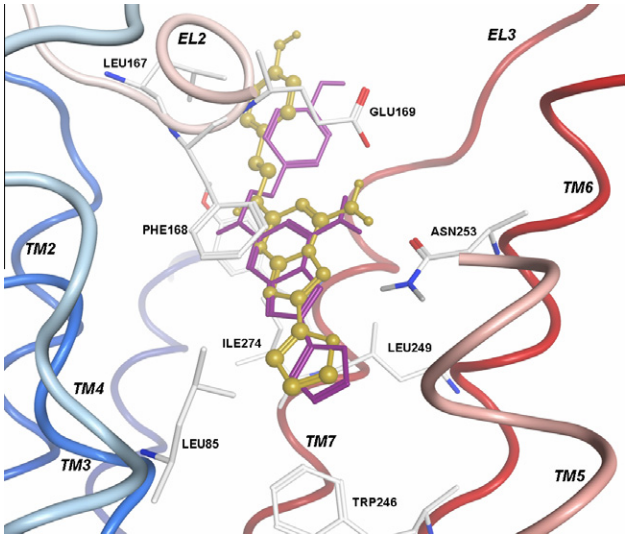

Figure 4. Validation of docking methodology by using the crystal structure of A_{2A}AR-ZM241385 complex. The X-ray binding mode of ZM241385 is taken as reference and displayed with 'stick style' in dark color. The predicted conformation of the same compound (after docking-minimization-rescoring processes) is shown with 'ball & stick style' in light color.

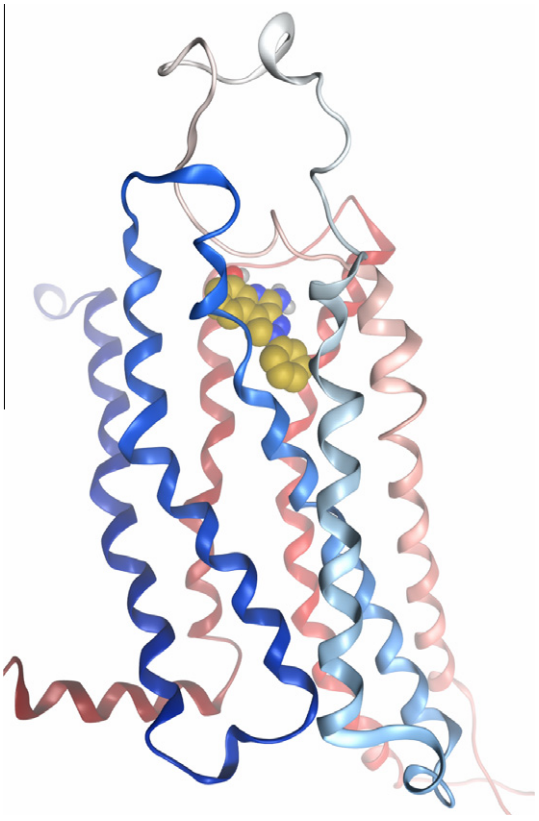

Figure 5. Homology model of A_1AR and binding mode of compound **9**.

ring that obstructs the second interaction. Similarly, in the binding mode of the pirazoloquinolines at A_1 and A_3 receptors only the 4-substituent seems to interact with the asparagine amide group (Asn254 and Asn250, respectively). To reduce the steric hindrance of the 2-moiety, the 2-phenyl ring (compounds **1A**, **1B**, **1** and **7**) was replaced with the smaller 2-methyl group (compounds **12–15**). This modification did not ameliorated the A_{2A} binding, the only exception being the 6-benzyloxy derivative **14** which showed an increased A_{2A} AR affinity (K_i = 750 nM), with respect to that corresponding 2-phenyl substituted derivative **7** (I% = 16). Replacement of the 2-phenyl moiety with the 2-methyl group was also detrimental for A_1 affinity. An analogous effect was already observed for 8-substituted adenine derivatives when tested at both human and rat A_1AR.[42] Given the high level of conservation of the above indicated hydrophobic subpocket among ARs, the opposite effect of 2-phenyl and 2-methyl substituents for AR affinity could be explained by hypothesizing slightly different volumes of the subpocket itself in the AR subtypes. As a consequence, the different effect of the 2-substituents on AR affinity could be related to their steric impact and to the different occupancy of the subpocket itself and not to specific ligand-receptor interactions.

Still considering the 4-group of the pyrazoloquinoline scaffold, docking conformations of these derivatives at A_1 and A_{2A} ARs present this group inserted between the above cited Asparagine 6.55 and a Glutamate residue conserved in both subtypes (Glu172 and Glu169, respectively, in A_1 and A_{2A} ARs). In the A_{2A}AR crystal structure, the carbonyl group of Asparagine amide and the carboxy function of Glutamate seem to both play a role as H-bond acceptor for the free amino group of ZM241385. This role is played also in the case of the 4-amino substituted pyrazoloquinolines and the importance of this interaction is particularly evident for binding to the A_{2A} AR. In fact, the only two compounds (**1B** and **14**) presenting nanomolar affinity, for this AR subtype, are substituted in the 4-position with a free amino group working as double H-bond donor. On the contrary, the presence of this pharmacophoric feature is not critical for the binding to the A_1 AR, as the pyrazoloquinolin-4-one derivative **1A** is endowed with higher affinity at this subtype, with respect to the 4-amino substituted analogue **1B**. The difference between the affinities of **1A** and **1B** is even more pronounced at the A_3 AR in which the Glutamate residue in EL2, conserved in A_1 (Glu172) and A_{2A} (Glu169), is replaced by a Valine (Val169). Hence the presence of a double H-bond donor group in the compound structure is not required (compare A_3AR affinity of compound **1A** to that of **1B**, Table 1) if not detrimental.[43] To interpret how the 4-oxo group of derivative **1A** can interact better than the amino group of **1B** with the Asparagine residue 6.55 of A_1 and A_3 ARs, the possible existence of the 4-oxo compound **1A** in the 4-enol form was evaluated. This hypothesis ensued from previously reported study on A_3AR antagonists belonging to the 4-oxo-substituted 1,2,4-triazolo[1,5-*a*]quinoxaline series.[19] This study suggested a possible 'tautomeric' selection made by the receptor binding site, with the keto form predicted as energetically more stable in solution and the enol form as fitting the binding site even better than the keto one.[19]

Enthalpies of formation of compound **1A** in keto and enol forms confirm the higher (~20 kcal/mol) stability of the first tautomer. Docking analysis of both forms at the three AR models shows that their binding modes are comparable to the one of 4-amino substituted compounds. Figure 6A shows the docking conformation of the enol tautomer of **1A** in the A_3 AR. Furthermore, the enol tautomer is observed to bind the three ARs also with a mirror orientation (Fig. 6B), that is with the 2-substituent located at the entrance of the binding site and the 6-position pointing towards the TM core region. In both cases, the enol polar hydrogen points towards the carbonyl group of Asparagine 6.55. Each scoring function used in our docking study presents comparable scores for both

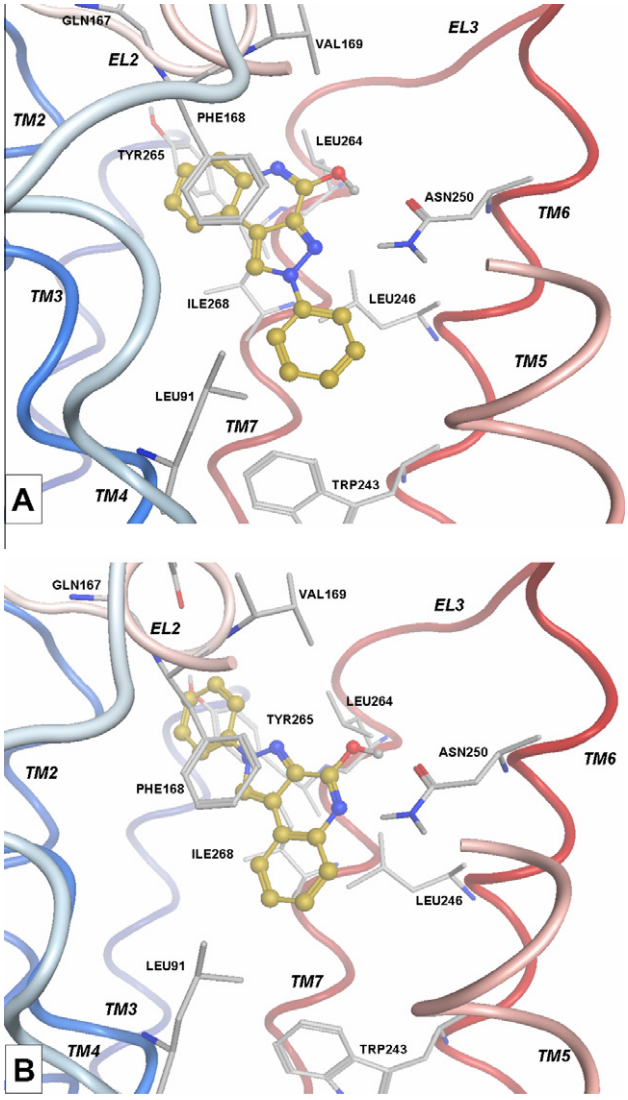

Figure 6. Binding modes of compound **1A** within A_3AR. EL2 is partially hidden for clarity. Receptor residues in ligand proximity are displayed.

binding modes of the enol form at the A_3 AR, suggesting that both ways of binding for this tautomer can occur at the A_3 AR. This data could explain the good A_3 AR affinity of compound **1A**.

Concerning the 6-substituent, it is positioned in proximity of A_1AR residues presenting a mainly polar/hydrophilic profile, such as Glu170 and Glu172 in EL2 segment and Thr270 and Tyr271 in TM7 domain. The corresponding residues in the A_{2A}AR are Leu167 and Glu169 in EL2 segment and Met270 and Tyr271 in TM7 domain, while in the A_3AR this subsection is defined by Gln170 and Val169 in EL2 segment and Leu264 and Tyr265 in TM7 domain. As a consequence, the chemical-physical profile of this region in A_{2A} and A_3 ARs is markedly less hydrophilic than that of the corresponding A_1 AR area. Thus, the presence of 6-substituents gives an increasing or decreasing contribution to AR affinity related to their chemical profile. In this sense, while 6-unsubstituted compound **1B** is endowed with higher affinity for the A_{2A}AR, with respect to the A_1 and A_3 ARs, its 6-hydroxy substituted analogue **9** presents an increased affinity for A_1 AR and a significant loss of binding to the other AR subtypes (Fig. 7).

Additional considerations can be made regarding the length and the nature of the 6-substituent. In particular, the nanomolar A_1 AR affinity of compound **7** (R_6 = OCH_2Ph) and the strong decrease of binding of its higher homolog **10** are explained by comparison of

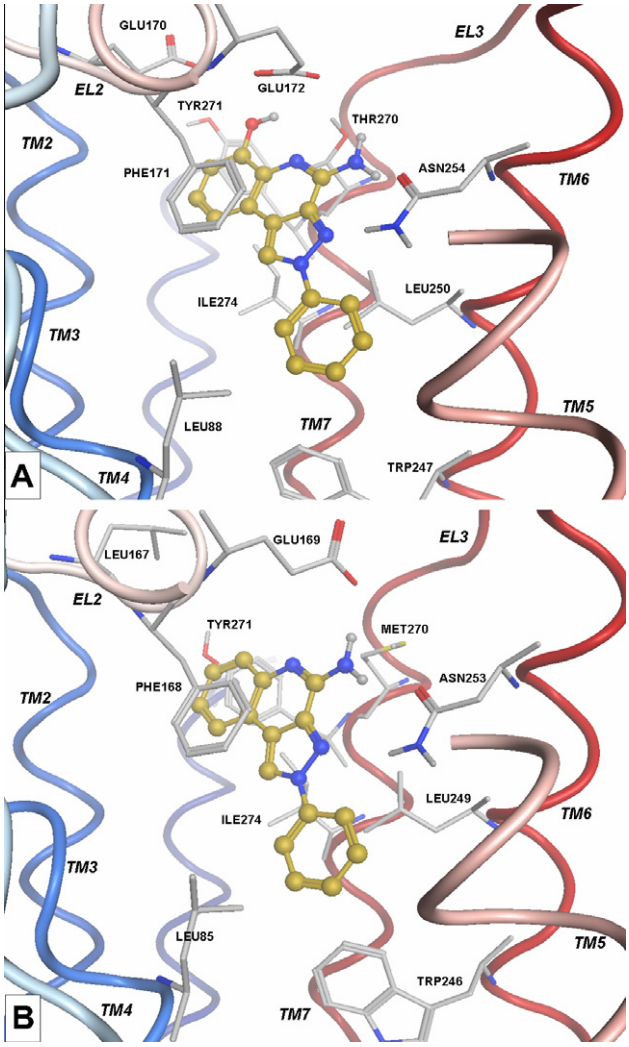

Figure 7. A and B: detailed view of binding mode of compound **9** within A_1AR and compound **1B** within A_{2A}AR, respectively. EL2 is partially hidden for clarity. Receptor residues in ligand proximity are displayed.

their docking conformations. The excessive length of the 6-substituent of compound **10** makes the phenyl ring being placed too exposed to the external of the receptor, and hence to the solvent, with a possible detrimental effect to receptor binding. On the other hand, comparison of binding modes and conformation energies of compounds **7** and **11** (R_6 = $NHCH_2Ph$) suggests that the presence of an amino group directly conjugated to the tricyclic scaffold provides more rigidity to the 6-substituent than an ether oxygen. As a consequence, while both derivatives are able to bind the A_1 AR, the slightly higher flexibility of the 6-substituent in compound **7** allows this molecule to fit the binding cavity with a more stable conformation than its analogue **11**.

5. Conclusion

The present work describes new 2-phenyl- and 2-methylpyrazolo[3,4-*c*]quinolin-4-ones (series **A**) and 4-amines (series **B**), bearing at the 6-position various groups with different lipophilicity and steric bulk. The 6-substituent was introduced with the aim of shifting affinities towards the A_1 and A_{2A} receptor subtypes. In series **A**, this modification was detrimental because it annulled the affinity of the parent compound **1A**. On the contrary, in series **B** it shifted affinity toward the A_1 receptor subtype. Indeed, most of the 2-phenylpyrazoloquinolin-4-amines showed an increased A_1 receptor affinity and selectivity, compared to those of the parent compound **1B**. Concerning the A_{2A} receptor, only the 2-methylpyrazoloquinolin-4-amine **14**, bearing the 6-benzyloxy moiety, showed some A_{2A} binding affinity. Docking results at A_1, A_{2A}, and A_3 AR binding sites highlighted the role of non-conserved receptor residues in the different interactions with the compound substituents whose effects on the AR affinity have been thus clarified. In conclusion, this study has provided new insights about the structural requirements of the AR antagonists belonging to the pyrazolo[3,4-*c*]quinoline series.

6. Experimental section

6.1. Chemistry

Silica gel plates (Merck F254) and silica gel 60 (Merck, 70–230 mesh) were used for analytical and column chromatography, respectively. All melting points were determined on a Gallenkamp melting point apparatus. Microanalyses were performed with a Perkin-Elmer 260 elemental analyzer for C, H, N, and the results were within ±0.4% of the theoretic values, unless otherwise stated. The IR spectra were recorded with a Perkin-Elmer Spectrum RX I spectrometer in Nujol mulls and are expressed in cm^{-1}. The ^1H NMR spectra were obtained with a Brucker Avance 400 MHz instrument. The chemical shifts are reported in δ (ppm) and are relative to the central peak of the solvent which was DMSO-d_6 or $CDCl_3$. The following abbreviations are used: s = singlet, d = doublet, t = triplet, m = multiplet, br = broad, and ar = aromatic protons. The mass spectra (MS) were acquired in positive mode over 100:600 *m*/*z* range using a Varian 1200L triple quadrupole mass spectrometer equipped with electrospray ionization (ESI) source.

6.1.1. General procedure for the synthesis of ethyl 7-substituted-3-indolylglyoxylates 20–23

Ethyl oxalyl chloride (2.24 mmol) was added to a solution of the commercially available 7-benzyloxyindole **16** and the suitably synthesized 7-R-indole derivatives **17**–**19**[29–31] (2.24 mmol) in anhydrous tetrahydrofuran (15 mL) and pyridine (4.48 mmol). The mixture was refluxed for 48 h, then the solid filtered off. The mother liquor was diluted with diethyl ether (about 20 mL) and the organic phase was washed twice with water (30 mL), anhydrified over Na_2SO_4 and evaporated to dryness at reduce pressure. The oily residue was taken up with cyclohexane (about 5 mL) to give a solid which was collected by filtration and recrystallized. Upon this treatment the 7-benzhydryloxy derivative **22** did not solidify, nevertheless the crude oil was pure enough to be used for the next step.

6.1.1.1. Ethyl (7-benzyloxy-1*H*-indol-3-yl)glyoxylate (20)[32]. Yield: 77%; mp 166–167 °C (cyclohexane/EtOAc). ^1H NMR ($CDCl_3$) 1.46 (t, 3H, CH_3, J = 7.1 Hz), 4.43 (q, 2H, CH_2, J = 7.1 Hz), 5.23 (s, 2H, CH_2), 6.89 (d, 1H, ar, J = 7.9 Hz), 7.29 (m, 1H, ar), 7.40–7.50 (m, 5H, ar), 8.05 (d, 1H, ar, J = 7.9 Hz), 8.43 (s, 1H, H-2), 9.05 (br s, 1H, NH). Anal. Calcd for $C_{19}H_{17}NO_4$: C, 70.58; H, 5.30; N, 4.33. Found: C, 70.31; H, 5.69; N, 4.01.

6.1.1.2. Ethyl (7-bromo-1*H*-indol-3-yl)glyoxylate (21)[33]. Yield: 70%; mp 151–153 °C (cyclohexane/EtOAc); ^1H NMR ($CDCl_3$) 1.46 (t, 3H, CH_3, J = 7.1 Hz), 4.42 (q, 2H, CH_2, J = 7.1 Hz), 7.24–7.26 (m, 1H, ar), 7.51 (d, 1H, ar, J = 7.8 Hz), 8.42 (d, 1H, ar, J = 8.0 Hz), 8.57 (s, 1H, H-2), 9.09 (br s, 1H, NH). Anal. Calcd for $C_{12}H_{10}BrNO_3$: C, 48.67; H, 3.40; N, 4.73. Found: C, 48.93; H, 3.73; N, 4.47.

6.1.1.3. Ethyl (7-benzhydryloxy-1*H*-indol-3-yl)glyoxylate (22). Yield: 78%; ^1H NMR ($CDCl_3$) 1.44 (t, 3H, CH_3, J = 7.2 Hz), 4.42 (q, 2H, CH_2, J = 7.2 Hz), 6.41 (s, 1H, CH), 6.71 (d, 1H, ar,

J = 7.9 Hz), 7.14 (t, 1H, ar, J = 8.0 Hz), 7.31–7.45 (m, 10H, ar), 8.00 (d, 1H, ar, J = 8.0 Hz), 8.43 (s, 1H, H-2), 9.15 (br s, 1H, NH). ESI-MS m/z calcd for $C_{25}H_{21}NO_4$: 399.2; found 400.2 $[M-H]^+$

6.1.1.4. Ethyl (7-benzyloxycarbonylamino-1*H*-indol-3-yl)glyoxylate (23). Yield: 55%; mp 211–213 °C. ^{1}H NMR ($CDCl_3$) 1.45 (t, 3H, CH_3, J = 7.2 Hz), 4.43 (q, 2H, CH_2, J = 7.2 Hz), 5.28 (s, 2H, CH_2), 6.80 (d, 1H, ar, J = 7.6 Hz), 7.22–7.28 (m, 2H, ar), 7.38–7.46 (m, 5H, ar), 8.29 (d, 1H, ar, J = 7.9 Hz), 8.46 (s, 1H, H-2), 11.08 (br s, 1H, NH). Anal. Calcd for $C_{20}H_{18}N_2O_5$: C, 65.25; H, 4.95; N, 7.65. Found: C, 65.25; H, 5.18; N, 7.92.

6.1.2. General procedure for the synthesis of 6-substituted 2,5-dihydro-2-phenyl-4*H*-pyrazolo[3,4-*c*]quinolin-4-ones 1–4

A suspension of phenylhydrazine hydrochloride (2.8 mmol) and the suitable ethyl 3-indolylglyoxylate **20**–**23** (1.4 mmol) in absolute ethanol (15 mL) and glacial acetic acid (2–3 drops) was heated at reflux until the disappearance of the starting material (TLC monitoring, 4–6 h). The mixture was cooled at room temperature and the solid was collected, washed with water and recrystallized. For compound **22**, no solid was obtained, thus the reaction mixture was worked up as follows. After cooling at room temperature, the solvent was evaporated under reduced pressure and the residue taken up with dichloromethane (about 70 mL). The solid was filtered off and the solvent evaporated to yield an oily residue which solidified after treatment with cyclohexane/diisopropyl ether. The crude solid was a mixture of the 6-benzylhydryloxy derivative **3** and of the 6-hydroxy compound **5**, which were separated by column chromatography (eluent cyclohexane/EtOAc/MeOH, 6:4:0.5).

6.1.2.1. 6-Benzyloxy-2,5-dihydro-2-phenyl-4*H*-pyrazolo[3,4-*c*]quinolin-4-one (1). Yield: 40%; mp 229–230 °C (acetonitrile). ^{1}H NMR (DMSO-d_6) 5.33 (s, 2H, CH_2), 7.14–7.20 (m, 2H, ar), 7.34–7.39 (m, 1H, ar), 7.47–7.64 (m, 8H, ar), 8.06 (d, 2H, ar, J = 7.9 Hz), 9.49 (s, 1H, H-1), 10.25 (s, 1H, NH); IR 1703. Anal. Calcd for $C_{23}H_{17}N_3O_2$: C, 75.19; H, 4.66; N, 11.44. Found: C, 75.38; H, 4.92; N, 11.15.

6.1.2.2. 6-Bromo-2,5-dihydro-2-phenyl-4*H*-pyrazolo[3,4-c]quinolin-4-one (2). Yield: 30%; mp 286–288 °C (2-ethoxyethanol). ^{1}H NMR (DMSO-d_6) 7.23 (t, 1H, ar, J = 7.9 Hz), 7.50 (t, 1H, ar, J = 7.4 Hz), 7.58–7.65 (m, 2H, ar), 7.73 (d, 1H, ar, J = 7.8 Hz), 8.02–8.05 (m, 3H, ar), 9.58 (s, 1H, H-1), 9.98 (s, 1H, NH). Anal. Calcd for $C_{16}H_{10}BrN_3O$: C, 56.49; H, 2.96; N,12.35. Found: C, 56.13; H, 2.68; N, 12.01.

6.1.2.3. 6-Benzhydryloxy-2,5-dihydro-2-phenyl-4*H*-pyrazolo[3,4-c]quinolin-4-one (3). Yield: 35%; mp 267–270 °C (acetonitrile). ^{1}H NMR (DMSO-d_6) 6.16 (br s, 1H, CH), 6.67 (d, 1H, ar, J = 8.1 Hz), 7.12–7.28 (m, 12H, ar), 7.46 (t, 1H, ar, J = 7.5 Hz), 7.62 (t, 2H, ar, J = 7.8 Hz), 8.05 (d, 2H, J = 7.8 Hz), 9.38 (br s, 1H, H-1); IR 1660. Anal. Calcd for $C_{29}H_{21}N_3O_2$: C, 78.54; H, 4.77; N, 9.47. Found: C, 78.30; H, 4.46; N, 9.68.

6.1.2.4. 6-Benzyloxycarbonylamino-2,5-dihydro-2-phenyl-4*H*-pyrazolo[3,4-*c*]quinolin-4-one (4). Yield: 38%; mp >300 °C (DMF). ^{1}H NMR (DMSO-d_6) 5.19 (s, 2H, CH_2), 7.25 (t, 1H, ar, J = 7.8 Hz), 7.36–7.62 (m, 9H, ar), 7.65 (d, 1H, ar, J = 7.2 Hz), 8.05 (d, 2H, ar, J = 7.9 Hz), 9.33 (br s, 1H, NH), 9.52 (s, 1H, H-1), 10.65 (br s, 1H, NH); IR 1730, 3250. Anal. Calcd for $C_{24}H_{18}N_4O_3$: C, 70.23; H, 4.42; N, 13.65. Found: C, 69.98; H, 4.74; N, 13.81.

6.1.3. Synthesis of 6-hydroxy-2,5-dihydro-2-phenyl-4*H*-pyrazolo[3,4-*c*]quinolin-4-one (5)

A suspension of compound **1** (2.72 mmol) in glacial acetic acid (10 mL) and 48% aqueous hydrobromic acid solution (10 mL) was refluxed for 15 min. The mixture was concentrated under reduced pressure and the residue solution (about 5 mL) was cooled at room temperature and diluted with water (15 mL). The solid was collected, washed with water and recrystallized. Yield 90%; mp 297–298 °C (EtOH). ^{1}H NMR (DMSO-d_6) 6.88 (d, 1H, ar, J = 7.9 Hz), 7.07 (t, 1H, ar, J = 7.8 Hz), 7.43–7.50 (m, 2H, ar), 7.63 (t, 2H, ar, J = 7.9 Hz), 8.05 (d, 2H, ar, J = 8.3 Hz), 9.45 (s, 1H, H-1), 9.99 (br s, 1H, OH or NH), 10. 29 (br s, 1H, OH or NH); IR 1654, 3368. Anal. Calcd for $C_{16}H_{11}N_3O_2$: C, 69.31; H, 4.00; N, 15.15. Found: C, 69.04; H, 4.32; N, 15.37.

6.1.4. Synthesis of 6-amino-2,5-dihydro-2-phenyl-4*H*-pyrazolo[3,4-*c*]quinolin-4-one (6)

Compound **4** (0.66 mmol) was dissolved in hot DMF (about 20 mL), then 10% Pd/C (30 mg) was added to the solution. The mixture was hydrogenated in a Parr apparatus, at 45 psi for 12 h. The catalyst was filtered off, the solution diluted with water (about 40 mL) and extracted with EtOAc (50 mL × 3 times). The organic phases were anhydrified (Na_2SO_4) and the solvent evaporated under reduced pressure. The residue was treated with water (a few mL) to yield a solid which was collected, washed with water and diethyl ether. Yield 82%; mp >300 °C (DMF). ^{1}H NMR (DMSO-d_6) 5.52 (s, 2H, NH_2), 6.73 (d, 1H, ar, J = 7.7 Hz), 6.97 (t, 1H, ar, J = 7.7 Hz), 7.23 (d, 1H, ar, J = 7.7 Hz), 7.43–7.48 (m, 1H, ar), 7.63 (t, 2H, ar, J = 7.6 Hz), 8.04 (d, 2H, ar, J = 7.6 Hz), 9.42 (s, 1H, H-1), 10.49 (br s, 1H, NH); IR 1677, 3193, 3379. Anal. Calcd for $C_{16}H_{12}N_4O$: C, 69.55; H, 4.38; N, 20.28. Found: C, 69.80; H, 4.12; N, 20.52.

6.1.5. General procedure for the synthesis of 6-substituted 4-chloro-2-phenyl-2*H*-pyrazolo[3,4-*c*]quinolines 24–26

A mixture of the 4-oxo derivatives **1**, **2**, and **4** (6.8 mmol) and phosphorous pentachloride (2.04 mmol) in phosphorous oxychloride (8 mL) was heated at reflux until the disappearance of the starting material (TLC monitoring, 15 min to 2 h). Evaporation of the excess of phosphorous oxychloride under reduced pressure gave an oil which after treatment with cold water (50 mL) yielded a solid that was collected, washed with water and dried. The 4-chloro derivatives **24**–**26** were unstable, thus they could not be re-crystallized. Nevertheless they were pure enough to be characterized (^{1}H NMR) and used without further purification.

6.1.5.1. 6-Benzyloxy-4-chloro-2-phenyl-2*H*-pyrazolo[3,4-*c*]quinoline (24). Yield 90%; ^{1}H NMR (DMSO-d_6) 5.35 (s, 2H, CH_2), 7.29–7.46 (m, 4H, ar), 7.53–7.69 (m, 6H, ar), 7.87 (d, 1H, ar, J = 7.8 Hz), 8.13 (d, 2H, ar, J = 7.9 Hz), 9.82 (s, 1H, H-1). ESI-MS m/z calcd for $C_{23}H_{16}ClN_3O$: 385.1; found 386.1 $[M-H]^+$.

6.1.5.2. 6-Bromo-4-chloro-2-phenyl-2*H*-pyrazolo[3,4-*c*]quinoline (25). Yield 98%; ^{1}H NMR (DMSO-d_6) 7.57–7.69 (m, 4H, ar), 8.02 (d, 1H, ar, J = 7.4 Hz), 8.14 (d, 2H, ar, J = 7.4 Hz), 8.35 (d, 1H, ar, J = 6.5 Hz), 9.92 (s, 1H, H-1). ESI-MS m/z calcd for $C_{16}H_9BrClN_3$: 356.9; found 357.9 $[M-H]^+$.

6.1.5.3. 6-Benzyloxycarbonylamino-4-chloro-2-phenyl-2*H*-pyrazolo[3,4-*c*]quinoline (26). Yield 90%; ^{1}H NMR (DMSO-d_6) 5.27 (s, 2H, CH_2), 7.37–7.73 (m, 9H, ar), 8.01 (d, 1H, ar, J = 7.8 Hz), 8.14 (d, 2H, ar, J = 7.7 Hz), 8.20 (d, 1H, ar, J = 7.9 Hz), 9.15 (s, 1H, NH), 9.87 (s, 1H, H-1). ESI-MS m/z calcd for $C_{24}H_{17}ClN_4O_2$: 428.1; found 429.1 $[M-H]^+$.

6.1.6. General procedure for the synthesis of 6-substituted 2-phenyl-2*H*-pyrazolo[3,2-*c*]quinolin-4-amines 7–8, 27–28

A mixture of the suitable 4-chloro derivative **24**–**26** (4.7 mmol) in absolute ethanol saturated with ammonia (15 mL) was heated

overnight at 120 °C in a sealed tube. The solid that precipitated upon cooling was collected, washed with water and recrystallized. Reaction of the 4-chloroderivative **26** afforded a mixture of the corresponding 4-amino derivative **27** and of the 6,4-diamino-substituted compound **28** which were separated by column chromatography (eluent cyclohexane/EtOAc/MeOH, 6:3.5:0.5). Compound **28** was not recrystallized, due to its scarce quantities. Thus, its melting point was not determined.

6.1.6.1. 6-Benzyloxy-2-phenyl-2*H*-pyrazolo[3,4-*c*]quinolin-4-amine (7). Yield 76%; mp 211–212 °C (MeOH/2-ethoxyethanol); ^{1}H NMR (DMSO-d_6) 5.26 (s, 2H, CH_2), 6.94 (br s, 2H, NH_2), 7.03 (d, 1H, ar, J = 7.1 Hz), 7.11–7.15 (m, 1H, ar), 7.33–7.53 (m, 6H, ar), 7.60–7.66 (m, 3H, ar), 8.11 (d, 2H, ar, J = 7.1 Hz), 9.47 (s, 1H, H-1); IR 1630, 3265, 3477. Anal. Calcd for $C_{23}H_{18}N_4O$: C, 75.39; H, 4.95; N, 15.29. Found: C, 75.62; H, 5.23; N, 15.52.

6.1.6.2. 6-Bromo-2-phenyl-2*H*-pyrazolo[3,4-*c*]quinolin-4-amine (8). Yield 65%; mp 233–235 °C (2-methoxymethanol); ^{1}H NMR (DMSO-d_6) 7.13 (t, 1H, ar, J = 7.1 Hz), 7.26 (br s, 2H, NH_2), 7.65 (t, 2H, ar, J = 7.9 Hz), 7.72 (t, 1H, ar, J = 6.9 Hz), 8.11 (d, 1H, ar, J = 7.9 Hz), 8.31 (d, 2H, ar, J = 7.9 Hz), 9.56 (s, 1H, H-1); IR 1631, 3294, 3474. Anal. Calcd for $C_{16}H_{11}BrN_4$: C, 56.66; H, 3.27; N, 16.52. Found: C, 56.40; H, 3.42; N, 16.85.

6.1.6.3. 6-Benzyloxycarbonylamino-2-phenyl-2*H*-pyrazolo[3,4-*c*]quinolin-4-amine (27). Yield 7%; mp 167–169 °C (cyclohexane/EtOAc); ^{1}H NMR (DMSO-d_6) 5.23 (s, 2H, CH_2), 7.20–7.32 (m, 3H, 1 ar + NH_2), 7.38–7.49 (m, 6H, ar), 7.51–7.69 (m, 3H, ar), 8.08–8.12 (m, 3H, ar), 9.15 (s, 1H, H-1), 9.51 (s, 1H, NH). Anal. Calcd for $C_{24}H_{19}N_5O_2$: C, 70.40; H, 4.68; N, 17.10. Found: C, 70.57; H, 4.45; N, 16.93.

6.1.6.4. 2-Phenyl-2*H*-pyrazolo[3,4-*c*]quinolin-4,6-diamine (28). Yield 20%; ^{1}H NMR (DMSO-d_6) 5.33 (br s, 2H, NH_2 at the 6-position), 6.68–6.71 (m, 3H, 1 ar + NH_2), 6.97 (t, 1H, ar, J = 7.7 Hz), 7.21 (d, 1H, ar, J = 7.5 Hz), 7.47–7.65 (m, 3H, ar), 8.11 (d, 2H, ar, J = 8.0 Hz), 9.39 (s, 1H, ar). ESI-MS m/z calcd for $C_{16}H_{13}N_5$: 275.1; found 276.1 $[M-H]^+$.

6.1.7. Synthesis of 6-hydroxy-2-phenyl-2*H*-pyrazolo[3,4-*c*]quinolin-4-amine (9)

10% Pd/C (80 mg) was added to a solution of compound **7** (2.3 mmol) in DMF (15 mL). The mixture was hydrogenated in a Parr apparatus for 3 h, at 35 psi, then the catalyst was filtered off. The solution was diluted with water (about 40 mL) to yield a solid which was collected by filtration and washed with water. The crude solid was purified by column chromatography (eluent cyclohexane/EtOAc/MeOH, 5:4.5:0.5). Yield 45%; mp 183–185 °C (acetonitrile); ^{1}H NMR (DMSO-d_6) 6.87 (d, 1H, ar, J = 7.8 Hz), 7.01 (br s, 2H, NH_2), 7.10 (t, 1H, ar, J = 7.8 Hz), 7.47–7.51 (m, 2H, ar), 7.62–7.66 (m, 2H, ar), 8.12 (d, 2H, ar, J = 7.6 Hz), 8.23 (br s, 1H, OH), 9.47 (s, 1H, H-1); IR 1620, 3348, 3461. Anal. Calcd for $C_{16}H_{12}N_4O$: C, 69.55; H, 4.38; N, 20.28. Found: C, 69.86; H, 4.07; N, 20.56.

6.1.8. Synthesis of 6-phenethoxy-2-phenyl-2*H*-pyrazolo[3,4-*c*]quinolin-4-amine (10)

A mixture of compound **9** (0.4 mmol), potassium carbonate (1.08 mmol), phenethyl bromide (1.08 mmol) in 2-butanone (10 mL) was heated at reflux for 48 h. After cooling at room temperature, the solid was filtered off and the solution concentrated to small volume (4–5 mL). The precipitated solid was collected, washed with water and recrystallized. Yield 30%; mp 228–230 °C (2-butanone); ^{1}H NMR (DMSO-d_6) 3.14 (t, 2H, CH_2, J = 7.3 Hz), 4.31 (t, 2H, CH_2, J = 7.3 Hz), 6.90 (br s, 2H, NH_2), 7.00 (d, 1H, ar, J = 7.9 Hz), 7.14 (t, 1H, ar, J = 8.1 Hz), 7.20–7.66 (m, 9H, ar), 8.10 (d, 2H, ar, J = 8.1 Hz), 9.47 (s, 1H, H-1). Anal. Calcd for $C_{24}H_{20}N_4O$: C, 75.77; H, 5.30; N, 14.73. Found: C, 75.39; H, 5.62; N, 14.91.

6.1.9. Synthesis of 6-benzylamino-2-phenyl-2*H*-pyrazolo[3,4-*c*]quinolin-4-amine (11)

A mixture of the 4,6-diammino derivative **28** (0.36 mmol), anhydrous zinc chloride (0.73 mmol), benzaldehyde (0.43 mmol) in anhydrous tetrahydrofuran (10 mL) was heated at reflux for 3 h. The suspension was cooled at room temperature and the solid collected by filtration, washed with water and then with diethyl ether. The crude Schiff base **29** was directly used for the next step. $NaBH_4$ (0.33 mmol) was added to a boiling suspension of **29** (0.16 mmol) in anhydrous methanol (7 mL). After 30 min, the solution was cooled at room temperature, diluted with water (5 mL) and stirred for 5 min. The solid was collected, washed with water and recrystallized. Yield 98%; mp 173–175 °C (MeOH/EtOH); ^{1}H NMR (DMSO-d_6) 4.46 (d, 2H, CH_2, J = 5.9 Hz), 6.28 (t, 1H, NH, J = 5.9 Hz), 6.52 (d, 1H, ar, J = 7.5 Hz), 6.82 (s, 2H, NH_2), 7.00 (t, 1H, ar, J = 7.7 Hz), 7.23–7.49 (m, 7H, ar), 7.63 (t, 2H, ar, J = 7.6 Hz), 8.11 (d, 2H, J = 8.0 Hz), 9.42 (s, 1H, H-1). Anal. Calcd for $C_{23}H_{19}N_5$: C, 75.59; H, 5.24; N, 19.16. Found: C, 75.32; H, 5.49; N, 18.96.

6.1.10. General procedure for the synthesis of 6-substituted 2,5-dihydro-2-methyl-4*H*-pyrazolo[3,4-*c*]quinolin-4-ones 12–13

The title compounds were prepared by reacting the suitable ethyl 3-indolylglyoxylate **20**[32] or **30**[35] (1.4 mmol) with methylhydrazine hydrochloride (2.8 mmol) in absolute ethanol (15 mL) and glacial acetic acid (2–3 drops). The mixture was heated at reflux for 24 h, then the solvent evaporated under reduced pressure. The residue was treated with water (about 20–30 mL) and the solid obtained was collected by filtration, washed with water and recrystallized.

6.1.10.1. 6-Benzyloxy-2,5-dihydro-2-methyl-4*H*-pyrazolo[3,4-*c*]quinolin-4-one (12). Yield 85%; mp 178–180 °C (MeOH); ^{1}H NMR (DMSO-d_6) 4.12 (s, 3H, CH_3), 5.31 (s, 2H, CH_2), 7.08–7.13 (m, 2H, ar), 7.31–7.46 (m, 4H, ar), 7.59 (m, 2H, ar, J = 7.32 Hz), 8.64 (s, 1H, H-1), 9.98 (br s, 1H, NH); IR 1665. Anal. Calcd for $C_{18}H_{15}N_3O_2$: C, 70.81; H, 4.95; N, 13.76. Found: C, 70.56; H, 4.62; N, 13.49.

6.1.10.2. 2,5-Dihydro-2-methyl-4*H*-pyrazolo[3,4-*c*]quinolin-4-one (13)[34]. Yield 40%; mp 284–286 °C (acetonitrile), lit 285–287 °C (MeOH); ^{1}H NMR (DMSO-d_6) 4.12 (s, 3H, CH_3), 7.15–7.19 (m, 1H, ar), 7.31–7.33 (m, 2H, ar), 7.86 (d, 1H, ar), 8.63 (s, 1H, H-1), 11.31 (br s, 1H, NH); IR 1665. Anal. Calcd for $C_{11}H_9N_3O$: C, 66.32; H, 4.55; N, 21.09. Found: C, 66.01; H, 4.83; N, 21.37.

6.1.11. Synthesis of 6-benzyloxy-4-chloro-2-methyl-2*H*-pyrazolo[3,4-*c*]quinoline (31)

A mixture of the 4-oxo derivatives **12** (6.8 mmol) and phosphorous pentachloride (2.04 mmol) in phosphorous oxychloride (8 mL) was heated at reflux for 3 h. Evaporation under reduced pressure of the excess of phosphorous oxychloride gave an oil which after treatment with cold water (50 mL) yielded a solid which was collected, washed with water and dried. The 4-chloro derivative **31** was unstable, nevertheless it was pure enough to be characterized (^{1}H NMR) and used without further purification. Yield 85%; ^{1}H NMR (DMSO-d_6) 4.29 (s, 3H, CH_3), 5.33 (s, 2H, CH_2), 7.24–7.56 (m, 7H, ar), 7.77 (d, 1H, ar, J = 7.6 Hz), 9.01 (s, 1H, H-1). ESI-MS m/z calcd for $C_{18}H_{14}ClN_3O$: 323.1; found 324.1 $[M-H]^+$.

6.1.12. Synthesis of 2-methyl-2*H*-pyrazolo[3,4-*c*]quinolin-4-amine (15)[36,37]

A mixture of the 4-oxo derivatives **13** (6.8 mmol) and phosphorous pentachloride (2.04 mmol) in phosphorous oxychloride (8 mL) was heated at reflux for 3 h. The oily residue, obtained from evaporation under reduced pressure of the excess of phosphorous oxychloride, was taken up with cyclohexane (40 mL) which was then evaporated under reduced pressure. This procedure was repeated again twice and the tarry residue was immediately used for the next step. The ^{1}H NMR (DMSO-d_6) spectrum of this residue is not reported since it showed the presence of a mixture of compounds. Thus the proton signals of the 4-chloro derivative **32** could not be unequivocally assigned. The tarry residue was taken up with absolute ethanol saturated with ammonia (15 mL) and the mixture heated at 110 °C for 12 h in a sealed tube. After cooling at room temperature, the solid was collected by filtration and washed with water. The 4-amino derivative **15** was purified by column chromatography (eluent CH_2Cl_2/MeOH, 9.5:0.5). Yield 16% (with respect to the starting 4-oxo derivative **32**); mp 210–212 °C; ^{1}H NMR (DMSO-d_6) 4.25 (s, 3H, CH_3), 6.74 (s, 2H, NH_2), 7.17 (t, 1H, ar, J = 7.6 Hz), 7.31 (t, 1H, ar, J = 7.7 Hz), 7.47 (d, 1H, ar, J = 8.1 Hz), 7.89 (d, 1H, ar, J = 7.7 Hz), 8.67 (s, 1H, H-1). Anal. Calcd for $C_{11}H_{10}N_4$: C, 66.65; H, 5.08; N, 28.26. Found: C, 66.38; H, 5.32; N, 28.54.

6.1.13. Synthesis of 6-benzyloxy-2-methyl-2*H*-pyrazolo[3,4-*c*]quinolin-4-amine (14)

A mixture of the 4-chloro derivative **31** (1.2 mmol) in absolute ethanol saturated with ammonia (15 mL) was heated overnight at 120 °C in a sealed tube. The solid that precipitated upon cooling was collected, washed with water and purified by column chromatography (eluent cyclohexane/EtOAc/MeOH, 2:6:2). Yield 55%; mp 239–241 °C (2-methoxyethanol); ^{1}H NMR (DMSO-d_6) 4.18 (s, 3H, CH_3), 5.24 (s, 2H, CH_2), 6.74 (br s, 2H, NH_2), 6.97 (d, 1H, ar, J = 7.4 Hz), 7.06 (t, 1H, ar, J = 7.9 Hz), 7.31–7.48 (m, 3H, ar), 7.51–7.53 (m, 3H, ar), 8.65 (s, 1H, H-1); IR 1641, 3271, 3479. Anal. Calcd for $C_{18}H_{16}N_4O$: C, 71.04; H, 5.30; N, 18.41. Found: C, 70.82; H, 5.61; N, 18.26.

6.2. Computational methodologies

All molecular modeling studies were performed on a 2 CPU (PIV 2.0–3.0 GHz) Linux PC. Homology modeling, energy minimization, and docking studies were carried out using Molecular Operating Environment (MOE, version 2009.10) suite.[44] All ligand structures were optimized using RHF/AM1 semiempirical calculations and the software package MOPAC implemented in MOE was utilized for these calculations.[41]

6.2.1. Human A_{2A}AR crystal structure refinement

The recently solved X-ray crystal structure of the hA_{2A}AR in complex with ZM241385 was retrieved from the RCSB Protein Data Bank (pdb code: 3EML; 2.6-Å resolution).[38] All hydrogen atoms were added, and the protein coordinates were then minimized with MOE using the AMBER99 force field.[45] The minimizations were performed by 1000 steps of steepest descent followed by conjugate gradient minimization until the RMS gradient of the potential energy was less than 0.05 kJ mol^{-1} Å^{-1}.

6.2.2. Homology modeling of the human A_1 and A_3 ARs

Homology models of the hA_1 and hA_3 ARs were built using the crystal structure of the hA_{2A}AR as template. The alignment of the AR primary sequences was built within MOE. The boundaries identified from the X-ray crystal structure of hA_{2A}AR were applied for the corresponding sequences of the TM helices of the hA_1 and hA_3 AR. The missing loop domains were built by the loop search method implemented in MOE. Once the heavy atoms were modelled, all hydrogen atoms were added, and the protein coordinates were then minimized with MOE using the AMBER99 force field. The minimizations were performed by 1000 steps of steepest descent followed by conjugate gradient minimization until the RMS gradient of the potential energy was less than 0.05 kJ mol^{-1} Å^{-1}. Reliability and quality of these models were checked using the Protein Geometry Monitor application within MOE, which provides a variety of stereochemical measurements for inspection of the structural quality in a given protein, like backbone bond lengths, angles and dihedrals, Ramachandran φ–ψ dihedral plots, and side chain rotamer and nonbonded contact quality.

6.2.3. Molecular docking analysis

All compound structures were docked into the A_1, A_{2A}, and A_3 AR binding site using the MOE Dock tool. This method is divided into a number of stages: *Conformational Analysis of ligands*. The algorithm generated conformations from a single 3D conformation by conducting a systematic search. In this way, all combinations of angles were created for each ligand. *Placement*. A collection of poses was generated from the pool of ligand conformations using Alpha Triangle placement method. Poses were generated by superposition of ligand atom triplets and triplet points in the receptor binding site. The receptor site points are alpha sphere centres which represent locations of tight packing. At each iteration a random conformation was selected, a random triplet of ligand atoms and a random triplet of alpha sphere centres were used to determine the pose. *Scoring*. Poses generated by the placement methodology were scored using two available methods implemented in MOE, the *London dG* scoring function which estimates the free energy of binding of the ligand from a given pose, and *Affinity dG* Scoring which estimates the enthalpic contribution to the free energy of binding. The top 30 poses for each ligand were output in a MOE database.

6.2.4. Post docking analysis

The five top-score docking poses of each compound were then subjected to energy minimization AMBER99 force field energy minimization until the RMS gradient of the potential energy was less than 0.05 kJ mol^{-1} Å^{-1}. Receptor residues within 6 Å distance from the ligand were left free to move, while the remaining receptor coordinates were kept fixed. In this phase, water molecules originally present in the hA_{2A}AR were recovered and subjected to energy minimization together with the ligands. AMBER99 partial charges of receptor and water molecules and MOPAC output partial charges of ligands were utilized. Once the compound-binding site energy minimization was completed, receptor coordinates were fixed and a second energy minimization stage was performed leaving free to move only compound atoms. MMFF94[46–52] force field was applied. For each compound, the minimized docking poses at A_1AR were then rescored using *London dG* and *Affinity dG* scoring functions and the *dock-pK_i* predictor. The latter tool allows estimating the pK_i for each ligand using the 'scoring.svl' script retrievable at the SVL exchange service (Chemical Computing Group, Inc. SVL exchange: http://svl.chemcomp.com). The algorithm is based on an empirical scoring function consisting of a directional hydrogen-bonding term, a directional hydrophobic interaction term, and an entropic term (ligand rotatable bonds immobilized in binding). For each compound, the top-score docking pose according to at least two out of three scoring functions was selected for final ligand-target interaction analysis.

6.3. Pharmacology

6.3.1. Human cloned A_1, A_{2A} and A_3 AR binding assay

All synthesized compounds were tested to evaluate their affinity at hA_1, hA_{2A} and hA_3 adenosine receptors. Displacement

experiments of [^{3}H]DPCPX (1 nM) to hA_1 CHO membranes (50 μg of protein/assay) and at least six to eight different concentrations of antagonists for 120 min at 25 °C in 50 mM Tris–HCl buffer pH 7.4 were performed.[53] Non specific binding was determined in the presence of 1 μM of DPCPX (⩽10% of the total binding). Binding of [^{3}H]ZM-241385 (1 nM) to hA_{2A}CHO membranes (50 μg of protein/assay) was performed using 50 mM Tris–HCl buffer, 10 mM $MgCl_2$ pH 7.4 and at least six to eight different concentrations of antagonists studied for an incubation time of 60 min at 4 °C.[54] Non specific binding was determined in the presence of 1 μM ZM241385 and was about 20% of total binding. Competition binding experiments to hA_3 CHO membranes (50 μg of protein/assay) and 0.5 nM [^{125}I]AB-MECA, 50 mM Tris–HCl buffer, 10 mM $MgCl_2$, 1 mM EDTA, pH 7.4 and at least six to eight different concentrations of examined ligands for 120 min at 4 °C.[55] Non-specific binding was defined as binding in the presence of 1 μM AB-MECA and was about 20% of total binding. Bound and free radioactivity were separated by filtering the assay mixture through Whatman GF/B glass fiber filters using a Brandel cell harvester. The filter bound radioactivity was counted by Scintillation Counter Packard Tri Carb 2810 TR with an efficiency of 62%.

6.3.2. Measurement of cyclic AMP levels in CHO cells transfected with hA_{2B}

CHO cells transfected with hA_{2B} subtype were washed with phosphate-buffered saline, diluted tripsine and centrifuged for 10 min at 200 g. The pellet containing the CHO cells (1×10^6 cells/assay) was suspended in 0.5 ml of incubation mixture (mM): NaCl 15, KCl 0.27, NaH_2PO_4 0.037, $MgSO_4$ 0.1, $CaCl_2$ 0.1, Hepes 0.01, $MgCl_2$ 1, glucose 0.5, pH 7.4 at 37 °C, 2 IU/ml adenosine deaminase and 4-(3-butoxy-4-methoxybenzyl)-2-imidazolidinone (Ro 20–1724) as phosphodiesterase inhibitor and preincubated for 10 min in a shaking bath at 37 °C. The potency of antagonists to A_{2B} ARs was determined by antagonism of NECA (200 nM)-induced stimulation of cyclic AMP levels. The reaction was terminated by the addition of cold 6% trichloroacetic acid (TCA). The TCA suspension was centrifuged at 2000*g* for 10 min at 4 °C and the supernatant was extracted four times with water saturated diethyl ether. The final aqueous solution was tested for cyclic AMP levels by a competition protein binding assay. Samples of cyclic AMP standard (0–10 pmol) were added to each test tube containing [^{3}H] cyclic AMP and the incubation buffer (trizma base 0.1 M, aminophylline 8.0 mM, 2-mercaptoethanol 6.0 mM, pH 7.4). The binding protein, previously prepared from beef adrenals, was added to the samples, incubated at 4 °C for 150 min, and after the addition of charcoal was centrifuged at 2000*g* for 10 min. The clear supernatant was counted in a Scintillation Counter Packard Tri Carb 2810 TR with an efficiency of 62%.[56]

6.3.3. Data analysis

The protein concentration was determined according to a Bio-Rad method[57] with bovine albumin as a standard reference. Inhibitory binding constant (K_i) values were calculated from those of IC_{50} according to Cheng & Prusoff equation $K_i = IC_{50}/(1+[C^*]/K_D^*)$, where [C*] is the concentration of the radioligand and K_D^* its dissociation constant.[58] A weighted non linear least-squares curve fitting program LIGAND[59] was used for computer analysis of inhibition experiments.

Acknowledgments

This work was supported by a grant of the Italian Ministry for University and research (MIUR, FIRB RBNE03YA3L project).

References and notes

1. Fredholm, B. B.; IJzerman, A. P.; Jacobson, K. A.; Klotz, K. N.; Linden, J. *Pharmacol. Rev.* **2001**, *53*, 527.
2. Jacobson, K. A.; Knutsen, L. J. S. In *Handb. Exp. Pharmacol.: Purinergic and Pyrimidinergic Signalling I*; Abbracchio, M. P., Williams, M., Eds.; Springer: Berlin, 2001; Vol. 151, p 129.
3. Ralevic, V.; Burnstock, G. *Pharmacol. Rev.* **1998**, *50*, 413.
4. Fredholm, B. B.; Arslan, G.; Halldner, L.; Kull, B.; Schulte, G.; Wasserman, W. *Naunyn-Schmiedeberg's Arch. Pharmacol.* **2000**, *362*, 364.
5. Fredholm, B. B.; Chern, Y.; Franco, R.; Sitkovsky, M. *Prog. Neurobiol.* **2007**, *83*, 263.
6. Maemoto, T.; Tada, M.; Mihara, T.; Ueyama, N.; Matsuoka, H.; Harada, K.; Yamaji, T.; Shirakawa, K.; Kuroda, S.; Akahane, A.; Iwashita, A.; Matsuoka, N.; Mutoh, S. *J. Pharmacol. Sci.* **2004**, *96*, 42.
7. Pinna, A. *Expert Opin. Invest. Drugs* **2009**, *18*, 1619.
8. Mihara, T.; Mihara, K.; Yarimizu, J.; Mitani, Y.; Matsuda, R.; Yamamoto, H.; Aoki, S.; Akahane, A.; Iwashita, A.; Matsuoka, N. *J. Pharmacol. Exp. Ther.* **2007**, *323*, 708.
9. Mihara, T.; Iwashita, A.; Matsuoka, N. *Behav. Brain Res.* **2008**, *194*, 152.
10. Baraldi, P. G.; Tabrizi, M. A.; Preti, D.; Bovero, A.; Fruttarolo, F.; Romagnoli, R.; Zaid, N. A.; Moorman, A. R.; Varani, K.; Borea, P. A. *J. Med. Chem.* **2005**, *48*, 5001.
11. Moro, S.; Gao, Z.-G.; Jacobson, K. A.; Spalluto, G. *Med. Chem. Rev.* **2006**, *26*, 131.
12. Kiesman, W. F.; Elzein, E.; Zablocki, J. In *Handbook of Experimental Pharmacology: Adenosine Receptors In Health and Disease*; Wilson, C. N., Mustafa, S. J., Eds.; Springer: Berlin, 2009; Vol. 193, pp 25–58.
13. Cristalli, G.; Müller, C. E.; Volpini, R. In *Handbook of Experimental Pharmacology: Adenosine Receptors In Health and Disease*; Wilson, C. N., Mustafa, S. J., Eds.; Springer: Berlin, 2009; Vol. 193, pp 59–98.
14. Kalla, R. V.; Zablocki, J.; Tabrizi, M. A.; Baraldi, P. G. In *Handbook of Experimental Pharmacology: Adenosine Receptors In Health and Disease*; Wilson, C. N., Mustafa, S. J., Eds.; Springer: Berlin, 2009; Vol. 193, pp 99–122.
15. Jacobson, K. A.; Klutz, A. M.; Tosh, D. K.; Ivanov, A. A.; Preti, D.; Baraldi, P. G. In *Handbook of Experimental Pharmacology: Adenosine Receptors In Health and Disease*; Wilson, C. N., Mustafa, S. J., Eds.; Springer: Berlin, 2009; Vol. 193, pp 123–159.
16. Colotta, V.; Catarzi, D.; Varano, F.; Cecchi, L.; Filacchioni, G.; Martini, C.; Trincavelli, L.; Lucacchini, A. *J. Med. Chem.* **2000**, *43*, 1158.
17. Colotta, V.; Catarzi, D.; Varano, F.; Cecchi, L.; Filacchioni, G.; Martini, C.; Trincavelli, L.; Lucacchini, A. *J. Med. Chem.* **2000**, *43*, 3118.
18. Colotta, V.; Catarzi, D.; Varano, F.; Calabri, F. R.; Lenzi, O.; Filacchioni, G.; Martini, C.; Trincavelli, L.; Deflorian, F.; Moro, S. *J. Med. Chem.* **2004**, *47*, 3580.
19. Catarzi, D.; Colotta, V.; Varano, F.; Lenzi, O.; Filacchioni, G.; Trincavelli, L.; Martini, C.; Montopoli, C.; Moro, S. *J. Med. Chem.* **2005**, *48*, 7932.
20. Lenzi, O.; Colotta, V.; Catarzi, D.; Varano, F.; Filacchioni, G.; Martini, C.; Trincavelli, L.; Ciampi, O.; Varani, K.; Marighetti, F.; Morizzo, E.; Moro, S. *J. Med. Chem.* **2006**, *49*, 3916.
21. Colotta, V.; Catarzi, D.; Varano, F.; Capelli, F.; Lenzi, O.; Filacchioni, G.; Martini, C.; Trincavelli, L.; Ciampi, O.; Pugliese, A. M.; Pedata, F.; Schiesaro, A.; Morizzo, E.; Moro, S. *J. Med. Chem.* **2007**, *50*, 4061.
22. Morizzo, E.; Capelli, F.; Lenzi, O.; Catarzi, D.; Varano, F.; Filacchioni, G.; Vincenzi, F.; Varani, K.; Borea, P. A.; Colotta, V.; Moro, S. *J. Med. Chem.* **2007**, *50*, 6596.
23. Colotta, V.; Capelli, F.; Lenzi, O.; Catarzi, D.; Varano, F.; Poli, D.; Vincenzi, F.; Varani, K.; Borea, P. A.; Dal Ben, D.; Volpini, R.; Cristalli, G.; Filacchioni, G. *Bioorg. Med. Chem.* **2009**, *17*, 401.
24. Colotta, V.; Lenzi, O.; Catarzi, D.; Varano, F.; Filacchioni, G.; Martini, C.; Trincavelli, L.; Ciampi, O.; Pugliese, A. M.; Traini, C.; Pedata, F.; Morizzo, E.; Moro, S. *J. Med. Chem.* **2009**, *52*, 2407.
25. Lenzi, O.; Colotta, V.; Catarzi, D.; Varano, F.; Poli, D.; Filacchioni, G.; Varani, K.; Vincenzi, F.; Borea, P. A.; Paoletta, S.; Morizzo, E.; Moro, S. *J. Med. Chem.* **2009**, *52*, 7640.
26. Baraldi, P. G.; Tabrizi, M. A.; Gessi, S.; Borea, P. A. *Chem. Rev.* **2008**, *108*, 238.
27. Chang, L. C.; Brussee, J.; IJzerman, A. P. *Chem. Biodivers.* **2004**, *1*, 1591.
28. Colotta, V.; Catarzi, D.; Varano, F.; Filacchioni, G.; Martini, C.; Trincavelli, L.; Lucacchini, A. *Bioorg. Med. Chem.* **2003**, *11*, 5509.
29. Bartoli, G.; Palmieri, G.; Bosco, M.; Dalpozzo, R. *Tetrahedron Lett.* **1989**, *30*, 2129.
30. Dobson, D.; Todd, A.; Gilmore, J. *Synth. Commun.* **1991**, *21*, 611.
31. Bell, M. G.; Gernert, D. L.; Grese, T. A.; Belvo, M. D.; Borromeo, P. S.; Kelley, S. A.; Kennedy, J. H.; Kolis, S. P.; Lander, P. A.; Richey, R.; Sharp, V. S.; Stephenson, G. A.; Williams, J. D.; Yu, H.; Zimmerman, K. M.; Steinberg, M. I.; Jadhav, P. K. *J. Med. Chem.* **2007**, *50*, 6443.
32. Sabatucci, J. P.; Demerson, C. A.; Failli, A. A. US 4810699 Patent, 1989.
33. Adachi, H.; Palaniappan, K. K.; Ivanov, A. A.; Bergman, N.; Gao, Z. G.; Jacobson, K. A. *J. Med. Chem.* **2007**, *50*, 1810.
34. Nagarajan, K.; Shah, R. K. *Indian J. Chem., Sect. B* **1992**, *31B*, 316.
35. Casnati, G.; Ricca, A. *Gazz. Chim. Ital.* **1963**, *93*, 355.
36. Hays, D. S.; Danielson, M. E.; Gerster, J. F.; Niwas, S.; Prince, R. B.; Kshirsagar, T. A.; Hepper, P. D.; Moser, W. H.; Moseman, J. T.; Radmer, M. R., Kavanagh, M. A.; Strong, S. A.; Bonk, J. D. U.S. Patent 20060100229, 2006.
37. Hays, D. S.; Danielson, M. E.; Gerster, J. F.; Niwas, S.; Prince, R. B.; Kshirsagar, T. A.; Hepper, P. D.; Moser, W. H.; Moseman, J. T.; Radmer, M. R., Kavanagh, M. A.; Strong, S. A.; Bonk, J. D. U.S. Patent 20090075980, 2009.

38. Jaakola, V. P.; Griffith, M. T.; Hanson, M. A.; Cherezov, V.; Chien, E. Y.; Lane, J. R.; IJzerman, A. P.; Stevens, R. C. *Science* **2008**, *322*, 1211.
39. Dal Ben, D.; Lambertucci, C.; Marucci, G.; Volpini, R.; Cristalli, G. *Curr. Top. Med. Chem.* **2010**, *10*, 993.
40. Costanzi, S.; Ivanov, A. A.; Tikhonova, I. G.; Jacobson, K. A. *Front. Drug Des. Discov.* **2007**, *3*, 63.
41. Stewart, J. J. *J. Comput. Aided Mol. Des.* **1990**, *4*, 1.
42. Volpini, R.; Dal Ben, D.; Lambertucci, C.; Marucci, G.; Mishra, R. C.; Ramadori, A. T.; Klotz, K. N.; Trincavelli, M. L.; Martini, C.; Cristalli, G. *ChemMedChem* **2009**, *4*, 1010.
43. Dal Ben, D.; Buccioni, M.; Lambertucci, C.; Marucci, G.; Thomas, A.; Volpini, R.; Cristalli, G. *Bioorg. Med. Chem.* **2010**, *18*, 7923.
44. Molecular Operating Environment; C.C.G., Inc., 1255 University St., Suite 1600, Montreal, Quebec, Canada, H3B 3X3.
45. Cornell, W. D.; Cieplak, P.; Bayly, C. I.; Gould, I. R.; Merz, K. M.; Ferguson, D. M.; Spellmeyer, D. C.; Fox, T.; Caldwell, J. W.; Kollman, P. A. *J. Am. Chem. Soc.* **1995**, *117*, 5179.
46. Halgren, T. A. *J. Comput. Chem.* **1996**, *17*, 490.
47. Halgren, T. A. *J. Comput. Chem.* **1996**, *17*, 520.
48. Halgren, T. A. *J. Comput. Chem.* **1996**, *17*, 553.
49. Halgren, T. A. *J. Comput. Chem.* **1996**, *17*, 587.
50. Halgren, T. A.; Nachbar, R. *J. Comput. Chem.* **1996**, *17*, 616.
51. Halgren, T. A. *J. Comput. Chem.* **1999**, *20*, 720.
52. Halgren, T. A. *J. Comput. Chem.* **1999**, *20*, 730.
53. Borea, P. A.; Dalpiaz, A.; Varani, K.; Gessi, S.; Gilli, G. *Life Sci.* **1996**, *59*, 1373.
54. Varani, K.; Rigamonti, D.; Sipione, S.; Camurri, A.; Borea, P. A.; Cattabeni, F.; Abbracchio, M. P.; Cattaneo, E. *FASEB J.* **2001**, *15*, 1245.
55. Varani, K.; Cacciari, B.; Baraldi, P. G.; Dionisotti, S.; Ongini, E.; Borea, P. A. *Life Sci.* **1998**, *63*, PL 81.
56. Varani, K.; Gessi, S.; Merighi, S.; Vincenzi, F.; Cattabriga, E.; Benini, A.; Klotz, K. N.; Baraldi, P. G.; Tabrizi, M. A.; Lennan, S. M.; Leung, E.; Borea, P. A. *Biochem. Pharmacol.* **2005**, *70*, 1601.
57. Bradford, M. M. *Anal. Biochem.* **1976**, *72*, 248.
58. Cheng, Y.; Prusoff, W. H. *Biochem. Pharmacol.* **1973**, *22*, 3099.
59. Munson, P. J.; Rodbard, D. *Anal. Biochem.* **1980**, *107*, 220.